

Thermoluminescence and Optically Stimulated Luminescence Properties of β -Irradiated $\text{TiO}_2\text{:Yb}$ Nanoparticles

M. Pal¹, U. Pal^{2,*}, V. Chernov³, R. Meléndrez³, and M. Barboza-Flores^{3,*}

¹ Posgrado en Ingeniería y Ciencias Aplicadas, UAEM-CIICAP, Cuernavaca, Morelos, México

² Instituto de Física, Benemérita Universidad Autónoma de Puebla, Apartado Postal J-48, Puebla, Puebla, 72570 Mexico

³ Centro de Investigación en Física, Universidad de Sonora, Apartado Postal 5-088, Hermosillo, Sonora, 83190 Mexico

The thermoluminescence (TL) and optically stimulated luminescence (OSL) response of $\text{TiO}_2\text{:Yb}$ nanoparticles are studied. After beta irradiation, the materials developed a significant TL/OSL signal associated to several localized trapping states around 360–620 K. The OSL signal is mainly due to the releasing of trapped charges in the low temperature (360 and 460 K) trapping states. A computer glow curve deconvolution procedure was used to determine the activation energies and kinetic order of the TL processes.

Keywords: TiO_2 Nanostructures, Thermoluminescence, Optically Stimulated Luminescence.

1. INTRODUCTION

Nanocrystalline materials display unusual chemical and physical properties that differ from those of the bulk materials and are promising for fabrication of novel nanodevices. A number of materials have been investigated as the host lattice for rare earth cations including oxides,^{1,2} sulfides,³ selenides,⁴ and metallorganic complexes.⁵ But in most of the cases, the final products have poor thermal stability and weak mechanical properties which prevent them from practical applications such as in solid state lasers and phosphor devices.⁶ The use of semiconductors such as ZnO ,⁷ TiO_2 ,^{8–11} ZnS ,¹² CdS ,³ CdSe ¹³ as host lattice for rare-earth (RE) doping is a good alternative, as their optical properties can be tuned or modified through doping. However, it is difficult to achieve effective doping due to the difference in ionic sizes of the host and dopant ions. In most of the cases, the rare-earth ions would be simply absorbed on the surface of the semiconductor particles revealing emissions related to the direct absorptions by the RE ions on the semiconductor surface instead of the energy transferred from the host lattice to dopant.

After the recent success of Yb doping in ZnO nanoparticles reported by our group,¹⁴ we prepared TiO_2 nanoparticles doped with Yb^{+3} ions. Though the ionic radius of Yb^{+3} ions (1.008 Å) is relatively larger than that of Ti^{+4}

ions (0.75 Å), there are a few reports on the successful doping of Yb in TiO_2 films.¹⁵ TiO_2 is a promising host material for lanthanide (Yb^{+3}) ions because of its high transparency in visible wavelength range and good thermal, chemical and mechanical properties. Moreover it is nontoxic, biocompatible material which is important for the application in medical field. Though TiO_2 has been used in paints, cosmetics, foodstuffs, toothpaste, chiclets, water purification process, etc.^{16–18} recently nanostructured TiO_2 is being utilized in designing tailored nanodevices like nanosensor, cell bioimaging, and biological contrast agents; with outstanding and novel applications in medicine.^{19,20}

The nanostructured ZnO:Yb developed through glycol mediated synthesis exhibited a good thermoluminescence (TL) and optically stimulated luminescence (OSL) response when exposed to beta radiation. Moreover, ZnO:Yb displayed a linear dose response in the 10–100 Gy dose range.¹⁴ The synthesis of nanostructured dosimetric material with high and reproducible TL/OSL sensitivity, good energy response and low TL/OSL losses, may open up new field of dosimetric application, relevant to medical and clinical radiotherapy. The efficacy of ZnO:Yb and YAG: (Ce, Tb) nanophosphors as TL/OSL dosimetric made pertinent to investigate others nanostructured materials.^{14,21} To this end, in the present paper, we report on the synthesis and TL/OSL properties of undoped and Yb doped TiO_2 nanoparticles. One of the main aims of

*Authors to whom correspondence should be addressed.

the present work is to develop high quality TL/OSL sensitive nanostructures, capable of achieving a dose assessment function under high-energy photon or charge particle exposures, which would be of obvious advantage in medical radiation nanodevices and nanotechnology.

2. EXPERIMENTAL DETAILS

TiO₂ nanoparticles were prepared through the controlled hydrolysis of titanium tetrabutoxide (Ti[O(CH₂)₃CH₃]₄ or TTB).²² First, 2.5 ml of TTB was dissolved in 25 ml of anhydrous ethanol under nitrogen atmosphere inside a glove box. The mixture was stirred vigorously for 30 minutes at room temperature, and then taken out from the glove box. The resulting solution was added drop-wise to 150 ml of deionized water adjusted to pH 3.8 with 0.1 M nitric acid under vigorous stirring. A white precipitate was formed almost immediately. The product was stored overnight at 2 °C in a refrigerator. The precipitate was separated from the reaction mixture by centrifugation and washed repeatedly with distilled water and ethanol to remove any existing precursor or side product and then dried at room temperature. For doping, YbCl₃·6H₂O (Alfa Aesar 99.9%) of 0.5, 2, 4 and 8 mol% (nominal) was added to the acidic water before drop-wise addition of the previously prepared TTB-ethanol mixture.

Morphology of the undoped and doped samples was studied using a JEOL JSM LV 5600 scanning electron microscope, with attached Noran SuprDry analytical system. Crystalline quality of the samples was studied by recording their X-ray diffraction (XRD) spectra in a Phillips X'Pert diffractometer using CuK α radiation ($\lambda = 1.5406 \text{ \AA}$). The composition of the samples was estimated through energy dispersive spectroscopy (EDS) measurements.

Beta irradiation was provided by a ⁹⁰Sr-⁹⁰Y source having an activity of 0.04 Ci and 5 Gy/min dose rate. The luminescence measurements were carried out on an automated Risø TL/OSL reader (model TL/OSL-DA-15). The heating rate of TL readouts was 2 K/s. OSL readouts were performed at RT by illumination with an IR laser (830 nm, about 0.4 W/cm² at 100% power). The recorded TL glow curves were analyzed by a home made deconvolution program based on the non-linear least-square Marquardt method.

3. RESULTS AND DISCUSSION

EDS spectra and estimated composition of the samples are presented in Figure 1 and Table I, respectively. Emission peaks belonging to O, Ti and Yb along with C peak appeared in the examined samples. The undoped sample contains extra stoichiometric Ti while the doped samples contain extra stoichiometric concentration of O. Such a high concentration of oxygen in the doped samples might

be indicative of partial oxidation of the Yb dopant. The EDS estimated Yb concentrations are proportional to the nominal doping levels of the samples. With the increase of nominal Yb concentration, more atom % of Yb was incorporated in the samples.

SEM micrographs of undoped and 8% Yb doped TiO₂ samples with corresponding particle size distribution histograms are shown in Figure 1. Quasi-spherical TiO₂ particles of sizes ranging 30–60 nm were formed in the samples. In general, the average size of the particles decreases with the increase of Yb doping concentration. X-ray diffraction studies (Fig. 2(a)) revealed that all the samples are mostly in amorphous form. Apparently, Yb does not affect the formation of partially crystalline rutile phase of TiO₂. The Yb doped TiO₂ powders are still in rutile phase (partly crystallized) as undoped sample. Figure 2(b) shows the amplified region of the (200) plane of the samples. The peak gradually shifts towards lower 2θ angle indicating the possible deformation of TiO₂ lattice due to Yb doping.

Figure 3(a) shows typical TL glow curves of undoped and Yb doped TiO₂ samples, after exposed to beta radiation at 300 Gy dose. The TL glow curves exhibit pronounced peak with the maximum at about 360 K, weak peak at about 430 K and some unstructured TL emissions at higher temperatures. The TL intensity of undoped Yb is higher than that of Yb doped samples except for 8% Yb doping. The TL glow peak structure reveals similar pattern, but their intensities vary from sample to sample. Moreover, these variations are not systematic with Yb concentration, which indicates the irregular influence of the doping on the TL properties of TiO₂ nanoparticles. Figure 3(b) shows the TL glow curves of the TiO₂ sample doped with 8% Yb recorded after irradiation with beta dose from 10 to 300 Gy. The integrated TL intensity increases almost linearly with irradiation dose. The shift of the maximum of 360 K peak to higher temperature (from 355 to 365 K) can be explained by destruction of the low temperature part of the peak during long irradiation times. At low dose, the 430 K TL peak appears itself as some unstructured feature, which becomes more pronounced as the dose increases. The TL between 470 and 620 K also increases proportionally to the irradiation dose, but its structure remains unresolved.

To clarify the structure of the TL glow curves a thermal cleaning procedure was carried out for the 8% Yb doped sample. The thermal cleaning consists in subsequent TL readouts after irradiation and preliminary heating up to an increasing end temperatures.²³ Figure 4(a) shows the TL glow curves recorded immediately after irradiation and after preheating, displayed as the logarithm of intensity versus reciprocal temperature scale. The behavior of the preheated glow curves is typical of a thermal cleaning procedure, showing the subsequent destruction of the 360 and 430 K peaks (low temperature side glow peaks)

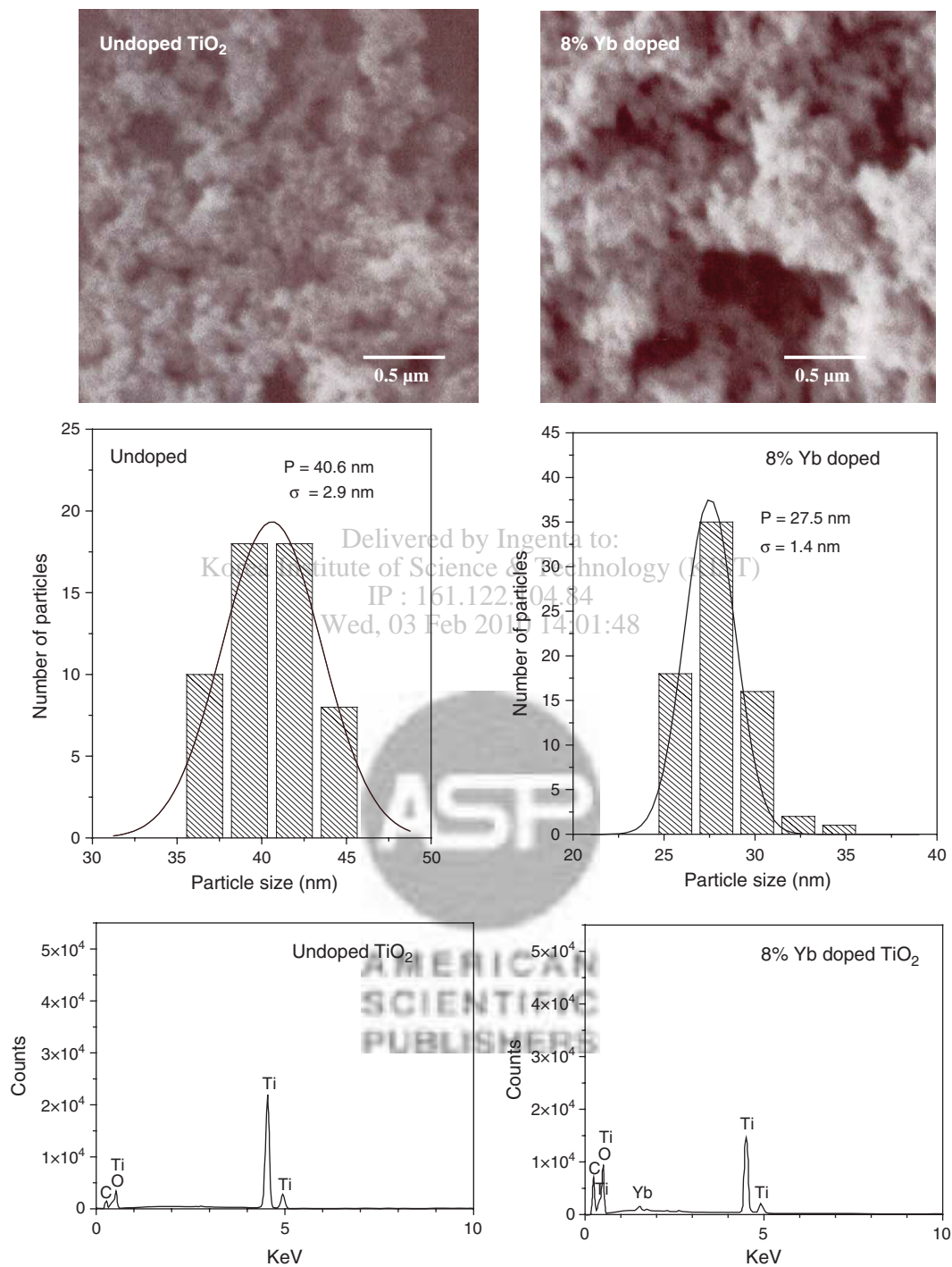


Fig. 1. Typical SEM micrographs, particle size distribution histograms and EDS spectra for the undoped (left) and 8% Yb (right) TiO₂ nanostructures.

along with a TL maximum shifting to higher temperatures. The maxima of the 360 and 430 K peaks are shifted to the high temperature region when the preheating temperature is increased. The initial parts of the glow curves are well described by straight lines that give a possibility to determine the activation energy by the initial rise method.²³ The dependence of the activation energy on the preheating temperature is shown in Figure 4(b). The first

(circles) and second (squares) sets of points correspond to the activation energies of traps responsible for the 360 and 430 TL peaks, respectively. The crosses show the activation energies determined for TL between 470 and 620 K. The activation energy of the 360 K peak monotonously increases from 0.9 to 1.1 eV with emptying of the traps by preliminary heating. The same situation is observed for the 430 K peaks, whose activation energy also increases from

Table I. EDS composition analysis of the undoped and Yb doped TiO₂ nanostructures.

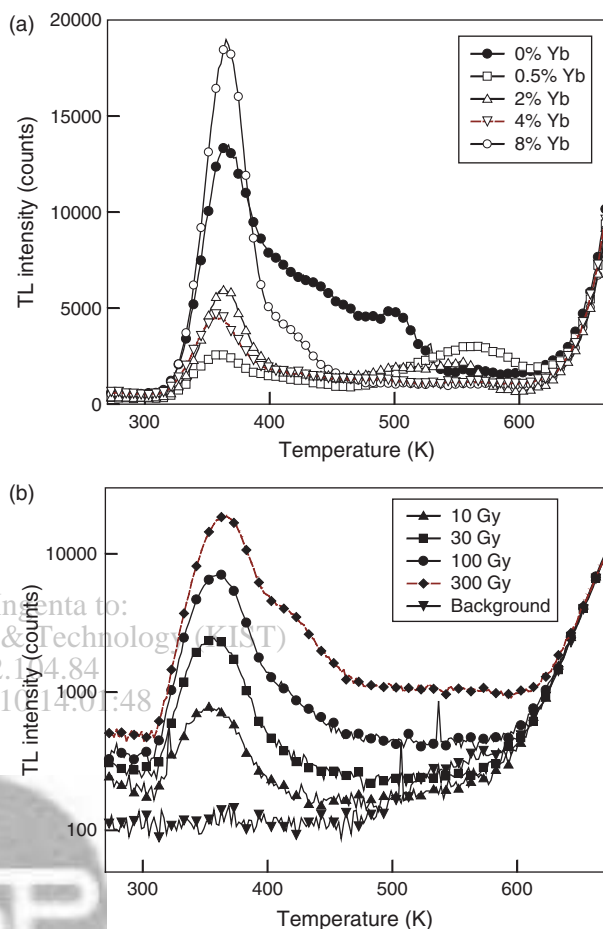
Sample	Atom %		
	Ti	O	Yb
TiO ₂ without doping	34.93	65.07	0.00
0.5 mol% Yb doped	26.00	73.68	0.32
2 mol% Yb doped	30.19	69.42	0.39
4 mol% Yb doped	26.11	73.42	0.47
8 mol% Yb doped	25.70	73.50	0.80

0.9 to 1.3 eV. The monotonous increasing of the activation energy clearly indicates that just one trapping level is not enough to explain the shape of the 360 or 430 K TL peaks. The activation energies of the traps responsible for the TL between 470 and 620 K vary from 1.1 and 1.25 eV.

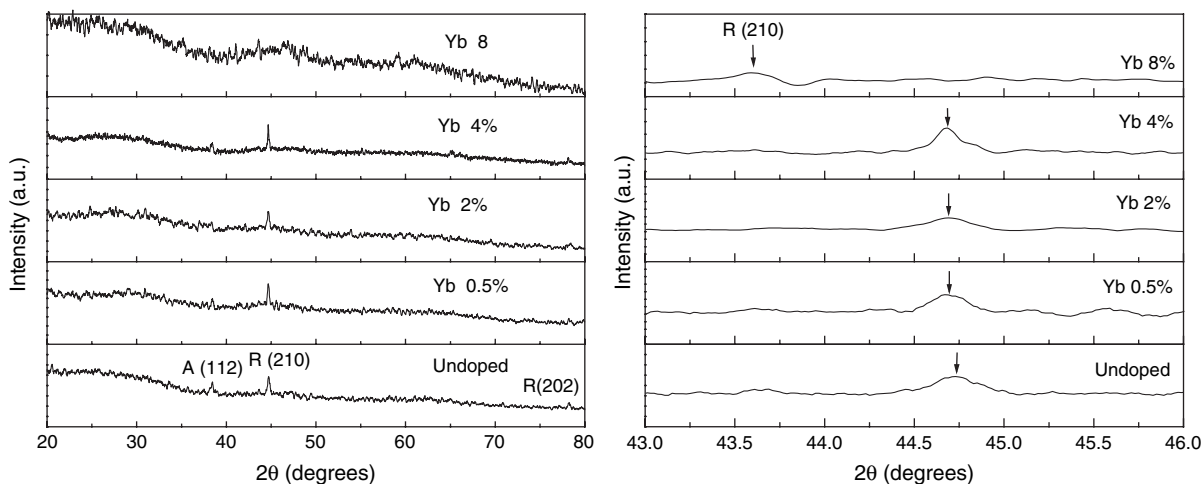
An alternative way to determine the kinetic parameters of the traps involved in the TL of an irradiated phosphor is to perform a computerized deconvolution of the TL glow curve on separate TL peaks components.²³ The broad high temperature side of the 360 the 430 K peaks, and the shift of their peak maxima during the cleaning procedure, indicate the existence of a second order kinetics process.²³ The equation describing the emptying of the filled TL traps for the second kinetics order can be written as:

$$S(T) = S_0 \left[1 + \frac{sk_B T^2}{\beta E} \exp\left(-\frac{E}{k_B T}\right) \left(1 - \frac{2k_B T}{E}\right) \right]^{-1} \quad (1)$$

Here, $S(T)$ represents the total light emitted during heating from temperature T up to a full emptying of the TL traps. The TL output $\Delta S(T)$ of the Risø TL/OSL system is proportional to some amount of light emitted during heating from temperature T to $T + \Delta T$. It can be represented as $\Delta S(T) = S(T) - S(T + \Delta T)$, and S_0 is the total TL yield emitted during the heating process (the peak area), E (eV) is the activation energy of the TL trap, s (s⁻¹) is the effective frequency factor (proportional to the frequency factor


Fig. 3. (a) TL glow curves of TiO₂:Yb samples as a function of Yb concentration exposed to 300 Gy beta ray dose; (b) TL glow curves of 8% Yb doped TiO₂ taken after beta irradiation at indicated doses.

of the TL trap with the proportional coefficient depending on the TL model used to derive the glow curve shape), β (Ks⁻¹) is the heating rate and k_B is the Boltzmann's constant.


Fig. 2. (a) X-ray diffraction patterns of the undoped and Yb doped TiO₂ nanostructures, and (b) the amplified region of the (200) plane.

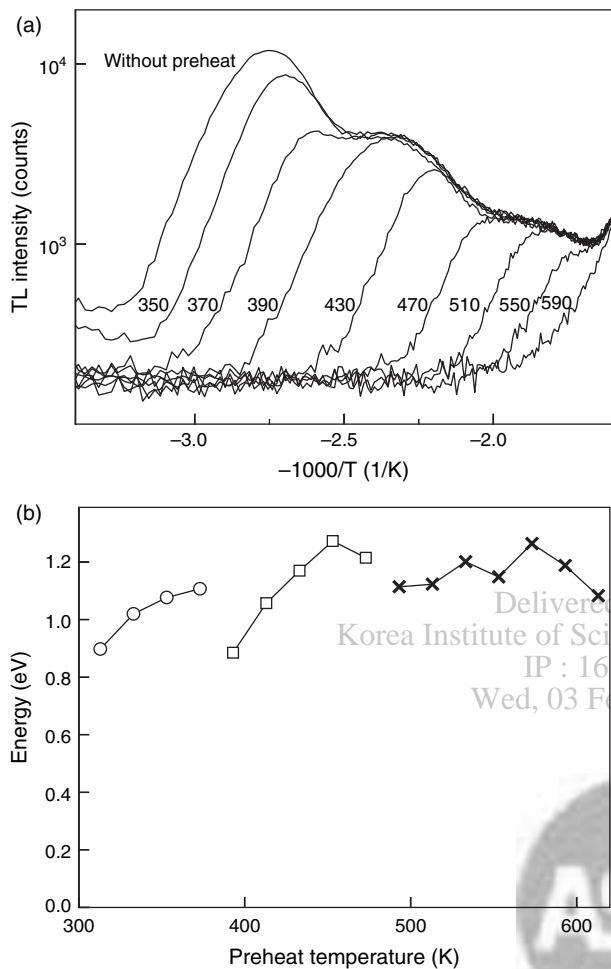


Fig. 4. (a) TL glow curves of 8% Yb doped TiO₂ after preliminary heating up to indicated temperatures (thermal cleaning) in the logarithm of intensity versus reciprocal temperature scales, and (b) the activation energy extracted from the initial slopes of the TL glow curves presented in figure (a). The circles, squares and crosses correspond to the 360 K peak, 430 K peak and higher temperature TL, respectively.

It should be mentioned that for significantly overlapped peaks, the deconvolution procedure is uncertain and several groupings of TL peak parameters can fit a glow curve with more or less equal accuracy. To overcome this difficulty, the activation energies were fixed during the deconvolution procedure. In accordance with the results of the initial rise method the 360 K peak, 430 K peak and TL between 470 and 620 K were supposed to consist of two second kinetics order peaks, each with the activation energies of 0.9 and 1.1 eV, 0.9 and 1.3 eV, 1.1 and 1.3 eV, respectively. The results of the deconvolution for undoped and 8% Yb doped TiO₂ samples are shown in Figure 5, which displays the experimental TL data along with the deconvoluted TL glow peak components (thin lines), including the residuals of the fitting process. It is possible to see that the experimental TL glow curves are described well by the combination of six peaks with the activation energies previously obtained with the

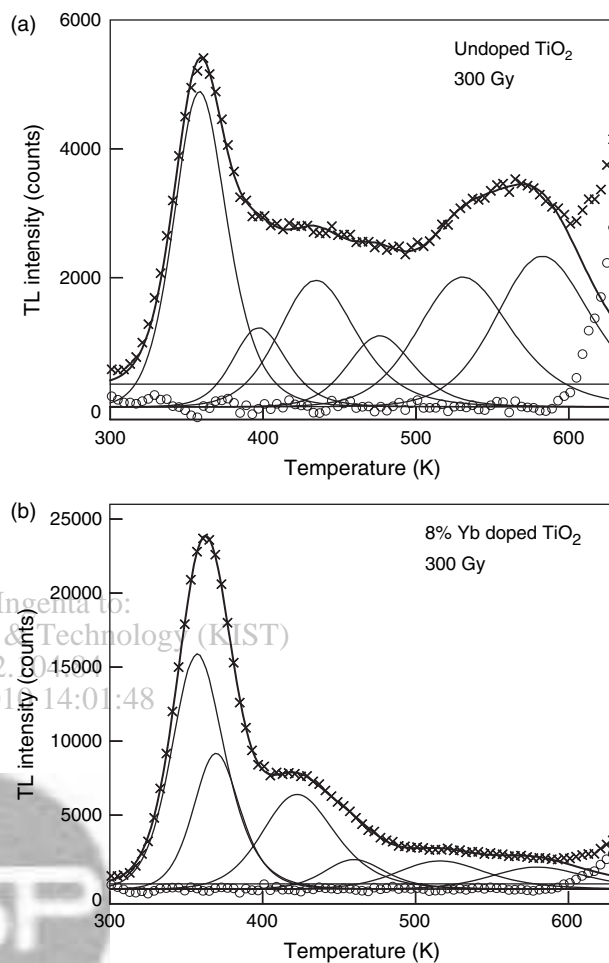


Fig. 5. Computer deconvolution of TL glow curves for (a) undoped TiO₂ and (b) 8% Yb doped TiO₂ nanostructures exposed to 300 Gy of beta radiation. The experimental TL curve is denoted by crosses; thin lines are the deconvoluted TL peaks and background, the bold line is the sum of the separate peaks and background; the circles are the residuals of the fitting process. The activation energies for the both curves are 0.9, 1.1, 0.9, 1.3, 1.1 and 1.3 eV, respectively.

thermal cleaning procedure. Of course, another arrangement of TL peaks with slightly different activation energies can describe these curves with the same precision. Nevertheless, in any case, we can conclude that the TL emissions in undoped and Yb doped TiO₂ are attributed to several traps whose activation energies lie within the range of 0.9–1.3 eV.

Figures 6(a) and 7(a) show the effect of stimulation with infrared light of 830 nm on the luminescence of undoped and 8% Yb doped TiO₂ samples, which were previously beta irradiated with 450 Gy dose. After irradiation exposure, the samples exhibit weak phosphorescence due to thermal emptying of the traps responsible for the 360 K TL peak. When the infrared stimulation is switched on, the luminescence intensity increases sharply due to liberation of trapped electrons from the traps by light. Further stimulation decreases the luminescence because of emptying of the traps. The OSL readout procedure (illumination

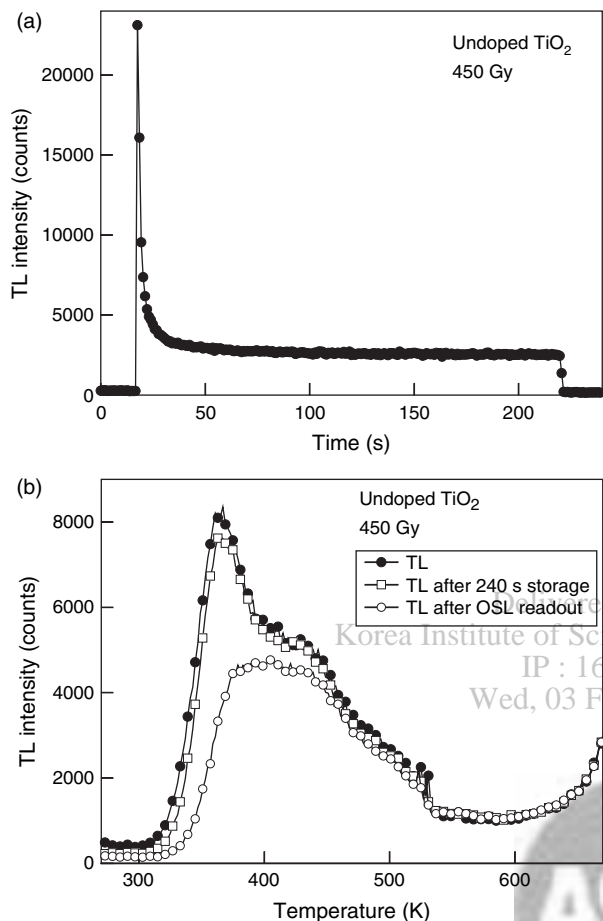


Fig. 6. Undoped TiO₂ sample exposed to 450 Gy beta radiations: (a) OSL decay curve, and (b) OSL readouts after storage in dark.

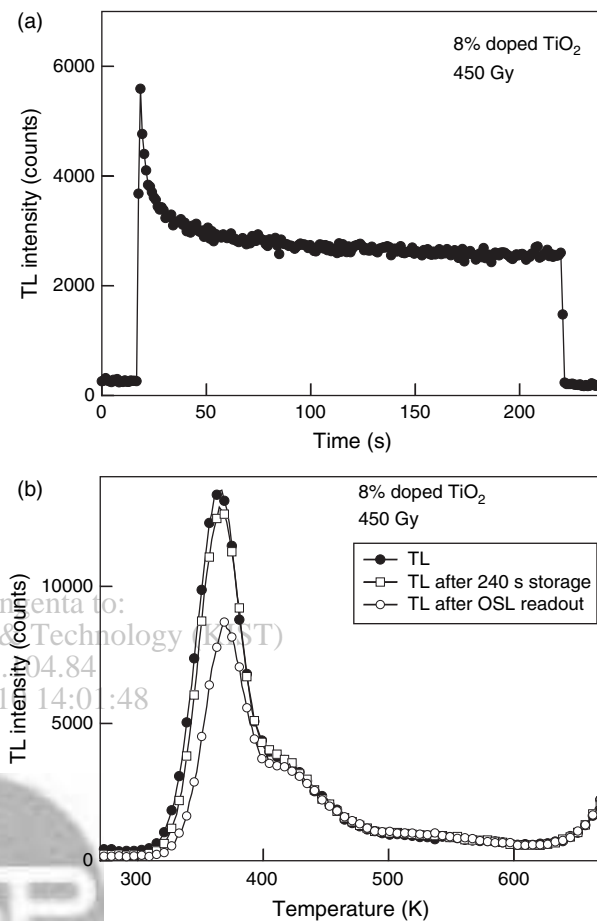


Fig. 7. 8% Yb doped TiO₂ sample exposed to 450 Gy beta radiations: (a) OSL decay curve, and (b) OSL readouts after storage in dark.

with infrared light) strongly influences the TL glow curves. Figures 6(b) and 7(b) show the TL curves recorded immediately after irradiation, after irradiation followed by storage in dark, and after irradiation followed by OSL IRSL readout. From the behavior of the TL glow curves it follows that trapped electrons are freed by heating and light. The release of trapped electrons at room temperature (thermal fading) is very weak and influences only the low temperature side of the 360 K TL peak. The release of trapped electrons induced by light stimulation is most pronounced for the 360 K TL peak and to some extent for the 430 K peak. The emptying of shallow localized trapping states by light stimulation is very common. However, it is somehow peculiar that infrared light does not destroy the high temperature TL peaks whose activation energies are close to those of the low temperature ones. It is interesting to mention that TL and OSL response of undoped and 8% doped samples are in inverse relation. That is, the doped sample has higher TL response while the undoped sample has higher OSL response. The reason of such behavior is not clear and further investigation on the matter is required.

During investigation of the nanostructured TiO₂ samples, two interesting features were observed. The first one is the very high sensitivity of the 2% Yb doped sample, which was observed at the beginning of the investigation, and its drastic decrease after one-month storage in darkness at room temperature (295 K). This situation is illustrated in Figure 8(a). The second feature is the observation of TL signal in un-irradiated samples. Figure 8(b) shows the TL glow curves measured in undoped TiO₂ which were preliminary heated up to 750 K and stored in the dark (inside the chamber of the TL/OSL reader) at indicated time. The glow curves exhibit a pronounced TL peak with a maximum at about 560 K whose intensity increases linearly with the storage time. The Yb doped samples exhibited similar behavior with a little different TL glow peaks. The origin of this TL emission for un-irradiated sample is not yet clear. However, a similar phenomenon was observed in the extensively used LiF:Mg, Ti TL dosimeters, which is associated to chemiluminescence caused by chemical reactions of oxygen with LiF surface. Therefore, it is possible that the TL build up in un-irradiated sample is also triggered by atmospheric water or oxygen interaction

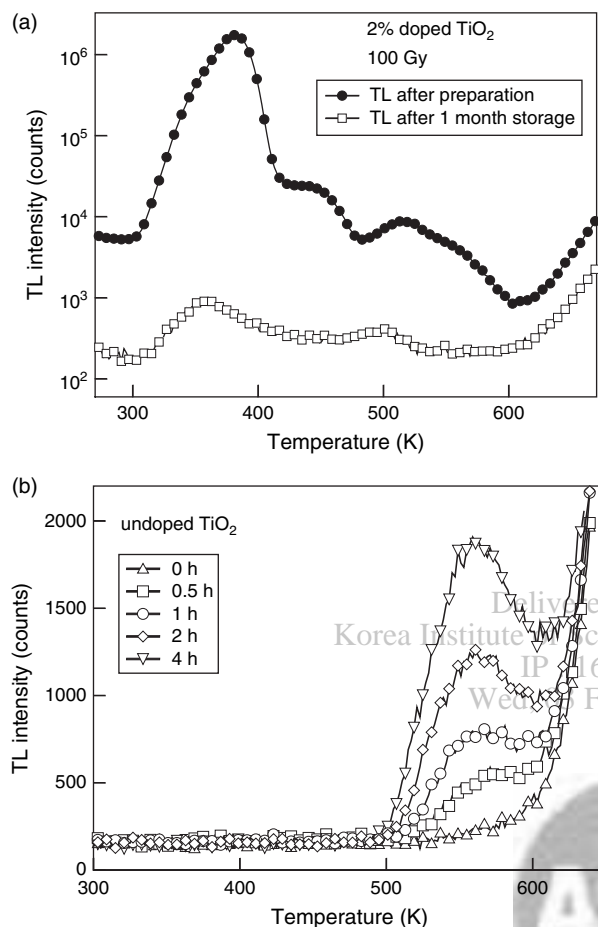


Fig. 8. (a) TL curves of 2% Yb doped TiO₂ sample exposed to 100 Gy beta radiations; after preparation and after one-month storage in laboratory conditions. (b) Increase of TL in undoped TiO₂ sample during storage in dark.

with our TiO₂:Yb nanoparticles. A detailed investigation on this peculiar phenomenon is in progress.

4. CONCLUSIONS

The present work reports results about the TL/OSL properties of beta irradiated spherical TiO₂:Yb nanoparticles of 30–60 nm in size, synthesized by controlled hydrolysis of titanium tetrabutoxide. The beta irradiated nanoparticles exhibit a good TL/OSL response depending irregularly on Yb doping concentration being higher for 8% Yb doping. The 360–620 K TL glow in undoped and Yb doped TiO₂ may be attributed to several localized trapping states with activation energies in the 0.9–1.3 eV range. The OSL response was found to be associated to the emptying of

the low temperature 360 K TL peak and partially to the 430 K peak. The present data, justifies further investigation on the TL/OSL phenomenon of the TiO₂:Yb nanoparticles to explore their TL/OSL behavior under high energy photon and particle beams irradiation dose assessments and delivery, which is of extreme importance in the medical diagnosis and radiotherapy fields.

Acknowledgments: We acknowledge UC-MEXUS and CONACyT, Mexico for their financial supports through Grants # CN-05-215 and # 46269, respectively.

References and Notes

1. D. K. Williams, B. Bihari, and B. M. Tissue, *J. Phys. Chem. B* 102, 916 (1998).
2. K. Riwotzki and M. Haase, *J. Phys. Chem. B* 102, 10129 (1998).
3. A. A. Bol, R. van Beek, and A. Meijerink, *Chem. Mater.* 14, 1121 (2002).
4. A. V. Firth, D. J. Cole-Hamilton, and J. W. Allen, *Appl. Phys. Lett.* 75, 3120 (1999).
5. J. Kido and Y. Okamoto, *Chem. Rev.* 102, 2357 (2002).
6. J.-G. Li, X. Wang, K. Watanabe, and T. Ishigaki, *J. Phys. Chem. B* 110, 1121 (2006).
7. Z. Zhou, T. Komori, M. Yoshino, M. Morinaga, N. Matsunami, A. Koizumi, and Y. Takeda, *Appl. Phys. Lett.* 86, 041107 (2005).
8. A. Conde-Gallardo, M. García-Rocha, I. Hernández-Calderón, and R. Palomino-Merino, *Appl. Phys. Lett.* 78, 3436 (2001).
9. S. Jeon and P. V. Braun, *Chem. Mater.* 15, 1256 (2003).
10. J. Ovenstone, P. J. Titler, R. Withnall, and J. Silver, *J. Phys. Chem. B* 105, 7170 (2001).
11. A. Patra, C. S. Friend, R. Kapoor, and P. N. Prasad, *Chem. Mater.* 15, 3650 (2003).
12. S. J. Xu, S. J. Chua, B. Liu, L. M. Gan, C. H. Chew, and G. Q. Xu, *Appl. Phys. Lett.* 73, 478 (1998).
13. X. Zhang, L. Liang, J. Zhang, and Q. Su, *Mater. Lett.* 59, 749 (2005).
14. U. Pal, R. Meléndrez, V. Chernov, and M. Barboza-Flores, *Appl. Phys. Lett.* 89, 183118 (2006).
15. W. W. Xu, S. Y. Dai, L. H. Hu, L. Y. Liang, and K. J. Wang, *Chinese Phys. Lett.* 23, 2288 (2006).
16. A. Kay and M. Grätzel, *Sol. Ener. Mater. Sol. Cel.* 44, 99 (1996).
17. W. Wang, B. Gu, L. Liang, W. A. Hamilton, and D. J. Wesolowski, *J. Phys. Chem. B* 108, 14789 (2004).
18. P. A. Mandelbaum, A. E. Regazzoni, M. A. Blesa, and S. A. Bilmes, *J. Phys. Chem. B* 103, 5505 (1999).
19. J. F. Hainfeld, D. N. Slatkin, and H. M. Smilowitz, *Phys. Med. Biol.* 49, N309 (2004).
20. S. H. Cho, *Phys. Med. Biol.* 50, N163 (2005).
21. E. De la Rosa, R. A. Rodríguez, R. Meléndrez, P. Salas, L. A. Diaz-Torres, and M. Barboza-Flores, *Nucl. Instr. and Meth. B* 255, 357 (2007).
22. W. Choi, A. Termin, and M. R. Hoffmann, *J. Phys. Chem.* 98, 13669 (1994).
23. R. Chen and S. W. S. McKeever, *Theory of Thermoluminescence and Related Phenomena*, World Scientific, Singapore (1997).

Received: 30 December 2007. Accepted: 12 March 2008.